World J Surg (2010) 34:2953–2959
DOI 10.1007/s00268-010-0764-1

World Journal of Surgery

Combined Use of Contrast-Enhanced Intraoperative Ultrasonography and a Fluorescence Navigation System for Identifying Hepatic Metastases

Kazuhisa Uchiyama · Masaki Ueno · Satoru Ozawa · Sigehisa Kiriyama · Yoshinobu Shigekawa · Hiroki Yamaue

Published online: 24 August 2010

Abstract
Background The purpose of this study was to assess the concomitant use of contrast-enhanced intraoperative ultrasound (CE-IOUS) using the new microbubble agent Sonazoid, and to assess the fluorescence navigation system (Photo Dynamic Eye, or PDE) using indocyanine green (ICG) as a novel tool for identifying colorectal metastatic lesions compared with preoperative contrast-enhanced multiple row-detected computed tomography (MDCT) and gadoxetic acid-enhanced MRI.
Methods Thirty-two patients who underwent a liver resection for colorectal metastatic carcinoma from 2008 to 2009 were included in the present study. ICG was intravenously injected within 2 weeks of the operation. The liver was inspected with CE-IOUS using Sonazoid and PDE for visualizing small metastatic lesions. A lesion analysis was performed with the postoperative histopathological examination of the resected tissues. The clinical values of CE-IOUS and PDE to confirm the malignant lesion diagnoses were statistically evaluated.
Results A total of 56 lesions were identified based on the histopathological findings of the biopsies and resected tissues; of these, 52 were confirmed to be metastases, whereas 4 were benign tumors. The numbers of identified metastases by MDCT/MRI and CE-IOUS/PDE were 46 and 51, respectively. The use of CE-IOUS and PDE improved the diagnostic sensitivity compared with the use of MDCT and EOB-MRI (98.1 vs. 88.5%, respectively; $P = 0.050$).
Conclusions The present results suggested that the concomitant use of CE-IOUS with the Sonazoid and PDE system may be a useful and safe method, in addition to CT or MRI.

K. Uchiyama · M. Ueno · S. Ozawa · S. Kiriyama · Y. Shigekawa · H. Yamaue (✉)
Second Department of Surgery, Wakayama Medical University School of Medicine, 811-1 Kimiidera, Wakayama 641-8510, Japan
e-mail: yamaue-h@wakayama-med.ac.jp

Introduction

Intraoperative fluorescent imaging techniques using indocyanine green (ICG) (Diagnogreen Inj., Daiichi Sankyo, Tokyo, Japan) have been used to detect sentinel lymph node metastases in patients with gastric, colon, and breast cancer [1, 2]. Recent studies have reported that liver tumors (hepatocellular carcinomas and metastatic carcinomas) exhibited strong fluorescence in patients who had been administered ICG several days before surgery for a routine preoperative liver function test [3, 4]. These techniques are based on the findings that ICG binds to plasma proteins, and protein-bound ICG emits light with a peak wavelength of approximately 830 nm when illuminated with near-infrared light [5].

Conventional intraoperative ultrasonography (IOUS) together with bimanual palpation has long been considered as the "gold standard" for assessing hepatic metastases. IOUS been shown to yield significant additional information not previously identified by preoperative imaging, which guides the resectability and the operative plan. Recently, contrast-enhanced IOUS (CE-IOUS) was performed using the new second-generation ultrasound microbubble agent Sonazoid (GE Healthcare, Oslo, Norway) to identify occult metastases during hepatectomy in patients with HCCs and liver metastases. The Sonazoid system provides a parenchyma-specific contrast image based on its accumulation in the Kupffer cells in the liver [6]. Sonazoid presents a late Kupffer-phase image with a long duration (approximately

2 h after injection) following vascular- and a sinusoidal-phase images. SonoVue (Bracco Spa, Milan, Italy) has been already used as a microbubble agent in CE-IOUS, but does not show the Kupffer-phase image [7]. The duration of the contrast enhancement of SonoVue was shorter, with a mean duration of 4 to 5 min. CE-IOUS using Sonazoid provided early vascular- and sinusoidal-phase images for 10 min followed by the late Kupffer-phase image up to 30 min after the injection.

Therefore, this study was designed to assess the added value of the concomitant use of CE-IOUS with Sonazoid and a fluorescence navigation system (PDE) using ICG as a novel tool for identifying metastatic lesions during liver resection. Although there are no reports of its concomitant use, this technique is simple and safe, and provides intraoperative information to improve the surgical outcome in these patients.

Patients and methods

Preoperative equipment

From 2008 to 2009, 32 consecutive patients (mean age, 71.8 (standard deviation (SD), 9.3) years; range, 28–82 years; 20 men and 12 women) were scheduled to undergo a liver resection due to liver metastasis. In all patients, enhanced CT and MRI imaging using the hepatocyte-targeted contrast agent gadolinium ethoxybenzyl diethylenetriamine penta acetic acid (Gd-EOB-DTPA; gadoxetic acid disodium, Primovist, Bayer Schering Pharma) was performed as previously described in a standardized preoperative examination 2 weeks before hepatic resection [8–10].

ICG was intravenously injected at a dose of 0.5 mg kg^{-1} body weight 2 weeks before surgery as part of a routine liver function test to determine the operative indications and procedures, and to exclude any patients with a history of an iodine allergy.

Intraoperative procedures

After exploration, the liver was routinely examined by CE-IDUS. The contrast agent Sonazoid (perflubutane microbubbles with a median diameter of 2–3 mm) was intravascularly injected at a dose of 0.0075 ml kg^{-1} by a manual bolus injection following a flush with 3.0 ml of normal saline. This contrast agent is characterized by the prolonged maintenance of its contrast attributes and allows continuous vascular and postvascular imaging. Microbubbles of the perflubutane-based contrast agent are phagocytosed by reticuloendothelial cells in the liver 10–30 min after injection, enhancing the liver parenchyma. CE-IOUS was performed upon ProSound α10 (Aloka Ltd., Tokyo, Japan) equipped with a micro-convex 3.5 MHz frequency probe. Immediately after the administration of Sonazoid, the portal veins, hepatic veins, and the normal liver parenchyma were uniformly enhanced except for the metastatic lesions, which were identified as dark contrast-free filling defects during an early vascular phase image lasting 3 min. The metastatic lesion was identified as a clear filling defect during a late Kupffer-phase image within 10–30 min after intravenous injection of Sonazoid.

The commercially available, near-infrared (NR) fluorescence imaging system (PDE; Hamamatsu Photonics K.K. Hamamatsu, Japan) activates ICG with emitted light at a wavelength of 760 nm and filters out light with wavelengths below 820 nm. The light source was a light-emitting diode (LED), and the detector was a charge-coupled device (CCD) camera. The fluorescence signals were sent to a digital video processor for display on a TV monitor. The PDE system is comprised of a small control unit (322- $\times$ 283- $\times$ 55-mm) and a camera unit (80- $\times$ 181- $\times$ 80-mm) for performing daily routine liver resections. Whereas ICG binds to human plasma, ICG is detectable as a fluorescence signal using an infrared observation camera system PDE. In our system, metastatic lesions located on the liver surface and at a finite depth of penetration into the scattering tissue, which limits detection to 5 mm from the surface, exhibited bright fluorescent signals and were easily detected by intraoperative PDE.

The statistical analyses were performed with a Chi-square test or Welch's t test, and statistical tests were two-sided, with a cutoff for statistical significance of $P < 0.05$. All patients were informed of the study design according to the Ethical Committee on Clinical Investigation of Wakayama Medical University Hospital and consented in writing to participate in this study.

Results

Tumor detection

A total of 56 lesions were identified by preoperative combined MDCT/MRI and combined CE-IOUS/PDE, including one lesion that was directly detected from the resected tissue. Of these 56 lesions, a total of 52 were considered malignant according to the postoperative histopathological examination and 4 were considered benign. Figure 1 shows a flowchart schematic illustration of the lesion detection in our study. Five additional malignant lesions were successfully identified by CE-IOUS/PDE. The number of histologically identified metastases on combined MDCT/MRI and combined CE-IOUS/PDE was 46 and 51, respectively (Table 1). Although one metastatic lesion was not detected by CE-IOUS/PDE, six malignant lesions were

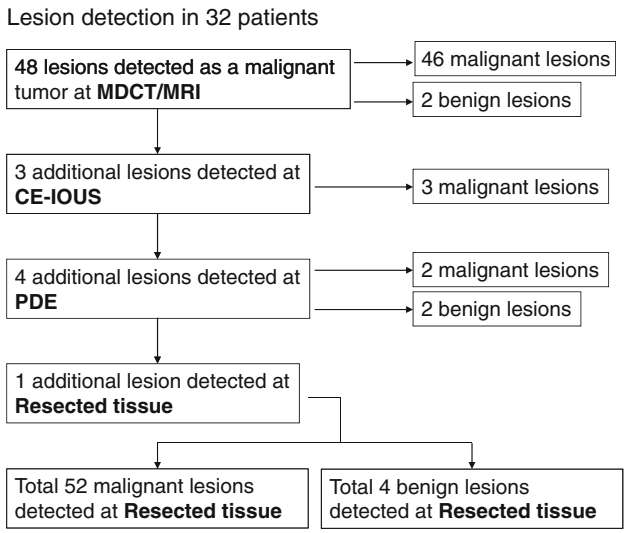

Fig. 1 Flowchart schema of lesion detection

Table 1 Malignant lesions diagnosed by MDCT/MRI and CE-IOUS/PDE

	No. of detected lesions	No. of not detected lesions	
Malignant lesions diagnosed by MDCT/MRI			
Hisotologically confirmed lesions			
Malignant lesions (*n*)	46	6	52
No malignant lesions (*n*)	2	0	2
	48	6	54
Malignant lesions diagnosed by CE-IOUS/PDE			
Hisotologically confirmed lesions			
Malignant lesions (*n*)	51	1	52
No malignant lesions (*n*)	2	0	2
	53	1	54

undetected by MDCT/MRI. The one missed lesion was only 3 mm in diameter and was detected at the cutting surface of the resected tissue. We mistook the metastatic lesion for the Glissonian branch. The use of concomitant CE-IOUS and PDE improved the malignant diagnostic sensitivity compared with the combination of preoperative MDCT and EOB-MRI (98.1 vs. 88.5%, respectively; $P = 0.050$; Table 2). With the use of CE-IOUS, three new lesions were identified in three patients, and the surgical strategy was changed in two of these patients. Intraoperative PDE identified four new lesions in three patients, and the surgical strategy was changed in two of these patients. One patient, who was planned to undergo posterior sectionectomy, instead underwent an additional partial wedge resection because of a newly identified lesion in Segment 2. The other patient underwent lateral sectionectomy and an additional partial resection of Segment 8.

Table 2 Summary of Results

	MDCT/MRI	CE-IOUS/PDE
Correctly identified metastases (*n*)	46	51
Sensitivity (%)	46/52 (88.5)	51/52 (98.1)*
Accuracy (%)	46/54 (85.2)	51/54 (94.4)
Positive predictive value (%)	46/48 (95.8)	51/53 (96.3)

* $P = 0.050$ compared with MDCT/MR

The median diameter of the detected malignant lesions was 18 (range, 8–62) mm for preoperative MDCT/MRI and 22 (range, 6–58) mm for CE-IOUS/PDE. The malignant lesions that were undetected by preoperative MDCT/MRI, but visible on CE-IOUS/PDE, had a median diameter of 7 (range, 4–11) mm.

Image characterization

CE-IOUS using Sonazoid contributed to the early vascular- and sinusoidal-phase images for 10 min, followed by the late Kupffer-phase image up to 30 min after injection. Figure 2 shows the IOUS and CE-IOUS images of a rectal carcinoma metastasis with liver cirrhosis at Segment 4. The metastatic lesion was unclearly detected as a slightly hypoechoic mass, which could not be differentiated from fibroid indurations based on the liver cirrhosis with IOUS; however, the CE-IOUS view of the same lesion was shown to be a clear hypoechoic mass at the late Kupffer-phase.

The intraoperative PDE imaging technique provides a broad, bright signal located in the metastatic lesion (Fig. 3). All 27 metastatic lesions, which were located at the liver surface, provided bright fluorescent signals and were easily detected by intraoperative PDE. The fluorescent patterns of the 27 metastatic lesions on the cut surfaces of the surgical specimens were categorized into the following three types: completely enhanced ($n = 5$; Fig. 3b), partially enhanced ($n = 4$), and ring enhanced ($n = 18$; Fig. 4c). The average diameter of the completely and partially enhanced-type metastasis was smaller than that of the ring enhanced type (8 ± 9 mm vs. 26 ± 21 mm, $P = 0.046$; Table 3). Nine of 27 lesions were detected as uniformly or partially fluorescent, whereas 18 of 27 lesions were detected as rim-fluorescing lesions with a low lesion-to-liver contrast. There was no relationship concerning the fluorescent imaging type and the histological differentiation of metastases. Although the small colorectal metastasis appeared to disappear with the MDCT image after the current chemotherapy as a modified FOLFOX6 (5-Fu, Leucovorin, Oxaliplatin, Bevacizumab; 6 cycle) (Fig. 4a, b), the lesion was found to exhibit bright ring fluorescent signals (Fig. 4c, d) using intraoperative PDE. This lesion was completely resected with negative margins under the guide

Fig. 2 IOUS and CE-IOUS images of a rectal carcinoma metastasis with liver cirrhosis at Segment 4. **a** Metastatic lesion was detected as a slightly hypoechoic mass, which could not be differentiated from the surrounding fibroid indurations, based on the liver cirrhosis. **b** CE-IOUS view of the same lesion revealed a clear hypoechoic mass at the late Kupffer-phase

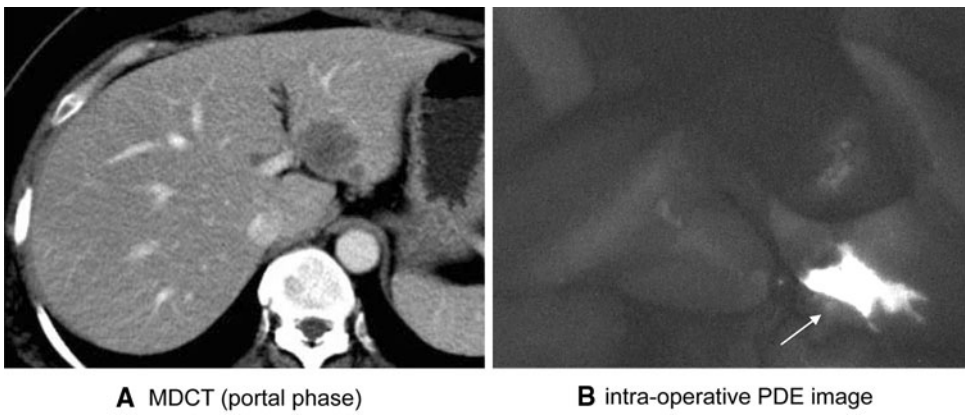

Fig. 3 Intraoperative ICG fluorescence imaging technique identified a broad, bright signal located in the metastatic lesion. **a** Metastatic lesion was confirmed with an interrupted low density mass at Segment 2 in the MDCT image (portal phase). **b** Intraoperative PDE image of the same lesion revealed a broad bright signal

of PDE, and several cancer cells (metastatic adenocarcinoma) were found by a postoperative histopathological examination.

Discussion

In the present study, we used combined triple-phase MDCT and CE-MRI with EOB as a standardized preoperative examination to decrease the false-positive rate. The numbers of false-positive CE-IOUS/PDE findings (3.7%) were the same as with those for triple-phase MDCT and CE-MRI with EOB (4.2%). The arterio-portal shunt is an important tumor mimicker that causes difficulty in the differentiation of small tumors in triple-phase MDCT scans [9]. However, as described in previous reports [10], none of the arterioportal shunts were hypointensive as analyzed by the EOB-MR image-enhanced hepatobiliary phase images. This finding may be helpful in differentiating the lesions from small tumors. Cirrhosis-related benign nodules may exhibit predominant hypoattenuation on contrast-enhanced portal or delayed phase CT images and may not be easily differentiated from hypovascular metastases [11]. However, the number of false-negative MRI findings was relatively low compared with the false-negative triple-phase MDCT findings [12].

SonoVue (Bracco Spa, Milan, Italy) has been already used as a microbubble agent in CE-IOUS, but the duration of the contrast enhancement was shorter, with a mean duration of 4–5 min. After the liver parenchymal enhancement had

Fig. 4 Change of the MDCT image 6 weeks after chemotherapy. **a**, **b** Metastatic lesion, which was located on the surface of Segment 5, was no longer detectable 6 months after chemotherapy (modified FOLFOX6). **c** Bright-rim fluorescent signals were present on the intraoperative PDE image. **d** The same bright rim fluorescent signals were observed in the resected tissue on the post-operative PDE image

Table 3 Fluorescent imaging type of the metastasis

Fluorescent type	No. of lesions	Tumor size (mm)	Histological differentiation Well:moderate
Totally enhanced type	5	8 ± 9*	5:4
Partially enhanced typi	4		
Ring enhanced type	18	26 ± 21	10:8

* $P = 0.046$ compared with Ring enhanced type

completely vanished (usually 5 min from the injection time), the injection of the same dose of SonoVue can be safely repeated (total safe dose per patient: 10 ml of SonoVue in 3 doses) to complete the examination [13], and we anticipate future software program optimization for improved sensitivity to contrast enhancement agents. The new injected perflubutane-based contrast agent Sonazoid is characterized by prolonged maintenance of its contrast attributes and allows continuous vascular and postvascular imaging. Microbubbles of the perflubutane-based contrast agent are phagocytosed by reticuloendothelial cells in the liver 10–30 min after injection, enhancing the liver parenchyma [14, 15]. Metastatic lesions appear as hypoechoic areas in the late Kupffer-phase of contrast-enhanced sonography, possibly because of the sparseness or absence of reticuloendothelial cells in colorectal metastatic lesions. Although there have been no reports about the median size of newly detected metastases identified by CE-IOUS with Sonazoid, the median size was identified on CE-IOUS with SonoVue, the prior generation contrast-enhanced drug, and was found to be 8 mm [13] and the smallest metastasis identified was 4 mm in diameter. The diameter of the lesions newly detected by CE-IOUS with SonoVue ranged from 2 to 11 mm [15], whereas in the present study using CE-IOUS/PDE, the median diameter of these lesions was 7 (range, 4–11) mm.

The concomitant use of CE-IOUS and PDE improved the diagnostic sensitivity compared with the combination of preoperative MDCT and EOB-MRI (98.1 vs. 88.5%, respectively; $P = 0.050$). With the addition of

CE-IOUS/PDE to preoperative MDCT/CE-MRI, five additional malignant lesions were successfully identified by CE-IOUS/PDE. The intraoperating PDE imaging system also was useful for identifying liver cancers, which were present on the liver surface [4]. ICG is a fluorescent dye given by intravenous injection for optical arteriography and the visualization of superficial vessels. Until now, intravenous ICG has been used as a routine preoperative liver functioning test and has not been associated with any major adverse effects apart from occasional allergic reactions. ICG-fluorescent imaging identified all microscopically confirmed liver metastases in the resected tumor specimens. There is a preferential accumulation of ICG in malignant or even benign nodules relative to the normal liver tissue, which is most likely due to biliary excretion disorders in the surrounding noncancerous liver tissues that have been compressed by the tumor. Nine of 27 lesions were detected as uniformly or partially fluorescing signals, whereas 18 of 27 lesions were detected as rim-fluorescing lesions with a low lesion-to-liver contrast. Macroscopically, fluorescence was present in the normal liver parenchyma surrounding the metastases. Ishizawa et al. [16] reported that well- or moderately differentiated hepatocellular carcinomas (HCCs) were detected as uniformly and highly fluorescing lesions, whereas poorly differentiated HCC and metastases were detected as rim-fluorescing lesions with a low lesion-to-liver contrast, thus suggesting that well- or moderately differentiated HCCs produces tumor fluorescence because cancer tissues retain the portal uptake of ICG, despite the functional and/or architectural destruction of biliary excretion due to cancer progression. In contrast, poorly differentiated HCCs and metastases produce rim fluorescence because of biliary excretion disorders in the surrounding normal liver tissues that have been compressed by the tumor. However, in the present findings, there was no relationship concerning the histological differentiation of metastases, most likely due to the small number of lesions that were examined.

Although our study population only consisted of 32 patients, we successfully performed liver resection using CE-IOUS/PDE in all patients. The role of the present system is important in chemotherapy-treated livers, and this technology appears to be promising for lesions that are not detectable by imaging and palpation alone. One metastatic lesion could not be differentiated from the surrounding fibroid indurations based on the liver cirrhosis with IOUS [17]; however, this lesion was observed as a clear hypoechoic image at the late Kupffer-phase with CE-IOUS using Sonazoid.

In conclusion, conventional intraoperative ultrasonography (IOUS) together with bimanual palpation has been considered the "gold standard" for assessing hepatic metastases, but the new CE-IOUS/PDE navigation method may be considered to be useful and safe for surgeons as an additional examination.

Conflicts of interest All authors and the Wakayama Medical University Hospital do not gain financially or otherwise by advertising this equipment, and report no conflicts of interest.

References

1. Noura S, Ohue M, Seki Y et al (2010) Feasibility of a lateral region sentinel node biopsy of lower rectal cancer guided by indocyanine green using a near-infrared camera system. Ann Surg Oncol 17:1 44–151
2. Murawa D, Hirche C, Dresel S et al (2009) Sentinel lymph node biopsy in breast cancer guided by indocyanine green fluorescence. Br J Surg 96:1289–1294
3. Aoki T, Yasuda D, Shimizu Y et al (2008) Image-guided liver mapping using fluorescence navigation system with indocyanine green for anatomical hepatic resection. World J Surg 32: 1763–1767
4. Gotoh K, Yamada T, Ishikawa O et al (2009) A novel image-guided surgery of hepatocellular carcinoma by indocyanine green fluorescence imaging navigation. J Surg Oncol 100:75–79
5. Kikuchi M, Hosokawa K (2009) Near-infrared fluorescence venography: a navigation system for varicose surgery. Dermatol Surg 35:1495–1498
6. Luo W, Numata K, Kondo M et al (2009) Sonazoid-enhanced ultrasonography for evaluation of the enhancement patterns of focal liver tumors in the late phase by intermittent imaging with a high mechanical index. J Ultrasound Med 28:439–448
7. Liu LP, Dong BW, Yu XL et al (2009) Focal hypoechoic tumors of Fatty liver: characterization of conventional and contrast-enhanced ultrasonography. J Ultrasound Med 28:1133–1142
8. Ueno M, Uchiyama K, Ozawa S et al (2009) A new prediction model of postoperative complications after major hepatectomy for hepatocellular carcinoma. Dig Surg 26:392–399
9. Zech CJ, Reiser MF, Herrmann KA (2009) Imaging of hepatocellular carcinoma by computed tomography and magnetic resonance imaging: state of the art. Dig Dis 27:114–124
10. Kim SH, Kim SH, Lee J et al (2009) Gadoxetic acid-enhanced MRI versus triple-phase MDCT for the preoperative detection of hepatocellular carcinoma. Am J Roentgenol 192:1675–1681
11. Marin D, Catalano C, De Filippis G et al (2009) Detection of hepatocellular carcinoma in patients with cirrhosis: added value of coronal reformations from isotropic voxels with 64-MDCT. AJR Am J Roentgenol 192:180–187
12. Zhao H, Yao JL, Wang Y et al (2007) Detection of small hepatocellular carcinoma: comparison of dynamic enhancement magnetic resonance imaging and multiphase multirow-detector helical CT scanning. World J Gastroenterol 13:1252–1256
13. Leen E, Ceccotti P, Moug SJ et al (2006) Potential value of contrast-enhanced intraoperative ultrasonography during partial hepatectomy for metastases: an essential investigation before resection? Ann Surg 243:236–240
14. Nakano H, Ishida Y, Hatakeyama T et al (2008) Contrast-enhanced intraoperative ultrasonography equipped with late Kupffer-phase image obtained by Sonazoid in patients with colorectal liver metastases. World J Gastroenterol 14:3207–3211
15. Miyamoto N, Hiramatsu K, Tsuchiya K et al (2009) Sonazoid-enhanced sonography for guiding radiofrequency ablation for hepatocellular carcinoma: better tumor visualization by Kupffer-phase

imaging and vascular-phase imaging after reinjection. Jpn J Radiol 27:185–193
16. Ishizawa T, Fukushima N, Shibahara J et al (2009) Real-time identification of liver cancers by using indocyanine green fluorescent imaging. Cancer 115:2491–2504
17. Torzilli G, Palmisano A, Del Fabbro D et al (2007) Contrast-enhanced intraoperative ultrasonography during surgery for hepatocellular carcinoma in liver cirrhosis: is it useful or useless? A prospective cohort study of our experience. Ann Surg Oncol 14:1347–1355